

The Fluid Dynamics of a Basaltic Magma Chamber Replenished by Influx of Hot, Dense Ultrabasic Magma

Herbert E. Huppert¹ and R. Stephen J. Sparks²

¹ Department of Applied Mathematics and Theoretical Physics, University of Cambridge, Silver Street, Cambridge CB3 9EW, England

² Department of Earth Sciences, Downing Site, University of Cambridge, Cambridge CB2 3EW, England

Abstract. This paper describes a fluid dynamical investigation of the influx of hot, dense ultrabasic magma into a reservoir containing lighter, fractionated basaltic magma. This situation is compared with that which develops when hot salty water is introduced under cold fresh water. Theoretical and empirical models for salt/water systems are adapted to develop a model for magmatic systems. A feature of the model is that the ultrabasic melt does not immediately mix with the basalt, but spreads out over the floor of the chamber, forming an independent layer. A non-turbulent interface forms between this layer and the overlying magma layer across which heat and mass are transferred by the process of molecular diffusion. Both layers convect vigorously as heat is transferred to the upper layer at a rate which greatly exceeds the heat lost to the surrounding country rock. The convection continues until the two layers have almost the same temperature. The compositions of the layers remain distinct due to the low diffusivity of mass compared to heat. The temperatures of the layers as functions of time and their cooling rate depend on their viscosities, their thermal properties, the density difference between the layers and their thicknesses. For a layer of ultrabasic melt (18% MgO) a few tens of metres thick at the base of a basaltic (10% MgO) magma chamber a few kilometres thick, the temperature of the layers will become nearly identical over a period of between a few months and a few years. During this time the turbulent convective velocities in the ultrabasic layer are far larger than the settling velocity of olivines which crystallise within the layer during cooling. Olivines only settle after the two layers have nearly reached thermal equilibrium. At this stage residual basaltic melt segregates as the olivines sediment in the lower layer. Depending on its density, the released basalt

can either mix convectively with the overlying basalt layer, or can continue as a separate layer. The model provides an explanation for large-scale cyclic layering in basic and ultrabasic intrusions. The model also suggests reasons for the restriction of erupted basaltic liquids to compositions with MgO < 10% and the formation of some quench textures in layered igneous rocks.

Introduction

High-level magma reservoirs within the Earth's crust are well known to undergo long-term chemical evolution as the chamber cools, becoming progressively more fractionated with time. Detailed petrological and geochemical studies of igneous rocks together with geophysical investigations of active volcanoes have provided persuasive evidence that many such magma chambers are periodically replenished by an influx of new and generally hotter primitive magma from depth.

The influx of new magma provides additional thermal energy to the chamber prolonging its life substantially (Usselman and Hodge 1978). The influx can also substantially modify the chemical fractionation of a magma chamber (O'Hara 1977), and provides a mechanism for eruption at the surface (Brown 1956; Sparks et al. 1977, 1980; Smith 1979). Evidence for replenishment can be found in all major volcanic environments: mid-ocean ridges (for example, Donaldson and Brown 1977; O'Hara 1977; Rhodes et al. 1977; Walker et al. 1979; Sparks et al. 1980); island arc volcanoes (Anderson 1976; Eichelberger 1978) and epicontinental silicic centres (Hildreth 1979; Smith 1979). There is also good evidence for the replenishment mechanism from the cyclic layering observed in many basic and ultrabasic in-

Reprint requests to: R.S.J. Sparks

trusive complexes (Brown 1956; Irvine and Smith 1967; Wager and Brown 1968; Irvine 1977; Smewing 1980). Magma chamber replenishment is evidently a process of major petrological importance.

In this paper we present a general treatment of the influx of hot, dense magma into the base of a magma chamber. Our treatment differs significantly from that presented by Usselman and Hodge (1978) in that we infer that the new magma does not immediately mix with the resident magma, but stratifies at the base of the chamber forming a two-layer system. The model treats the cooling history of the two turbulently convecting layers as they exchange heat across a nonturbulent interface.

The model is applied to the case of a picritic basalt magma intruded into a chamber containing fractionated basalt. We discuss features of basic and ultrabasic rocks which can be explained in terms of the model. We reinterpret the large-scale cyclic layering observed in the ultrabasic parts of layered intrusions such as Rhum and at the base of many ophiolite complexes. We also discuss the scarcity of highly magnesian liquids ($\text{MgO} > 10.0\%$) in eruptive suites and the tendency for tholeiitic basalts to fall in a restricted compositional range.

General Assumptions

Figure 1 shows a basaltic magma chamber filled with fractionated magma. The model we develop employs a simple rectangular shape for the chamber (Fig. 1b), which is sufficient to elucidate the fundamentals of the phenomena under investigation. The magma evolves chemically as heat is lost resulting in crystal fractionation which is usually assumed to be the dominant process in basaltic magmas.

We assume that new melt is introduced from depth into the reservoir and that the influx is geologically instantaneous. Explicitly, we assume that the time taken for the influx is small – less than a few weeks – compared to the thermal decay time of months or years, which we calculate for the system. Different fluid mechanical concepts are involved if the magma leaks into the reservoir continually, which is a possible alternative. We assume that the new magma is hotter, but denser than the resident magma. In the case of basic and ultrabasic melts, the larger density of the new magma is due to its increased normative olivine content.

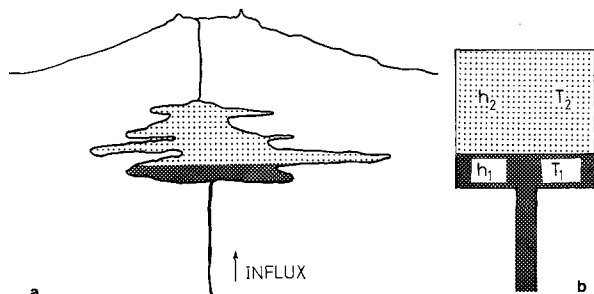


Fig. 1. a High-level magma chamber beneath a volcano. b A simplified model of the chamber

In the simplified chamber (Fig. 1b) the new liquid, because of its higher density, stratifies at the base of the chamber with thickness h_1 and temperature T_1 . The main part of the chamber is still occupied by pre-existing magma with thickness h_2 and temperature T_2 . The model treats the cooling history of the two layers. There are physical controls on the relative thickness of the two layers. If the surrounding country rock does not fracture, then the amount of new liquid capable of entering the chamber is restricted by the elastic deformation of the chamber walls and the compressibility of the magma itself. If the country rocks fracture, however, then magma from the chamber can be intruded to form dykes or erupted at the surface making room for the incoming liquid.

An important factor in the development of a model is to decide on the nature of the interface between the two liquids. Studies of the convection that occurs when a layer of hot, salty water lies beneath a relatively colder, fresher and lighter layer indicate that the transfer of heat and salt through the interface is entirely by the process of molecular diffusion, even though each layer is in vigorous convective motion (Turner 1979). This passive structure of the interface relies on the different molecular diffusivities of heat and salt. Experiments with heat and salt, or with different pairs of quantities, for example with two solutes of different molecular diffusivities, confirm that little matter is directly transferred from one layer to the other by turbulent eddies. The quantitative relationships for the rates of transfer of heat and salt obtained in the laboratory for this double-diffusive system have been confirmed to hold in larger-scale, natural systems. Huppert and Turner (1972) tested these relationships by developing a thermal model of a salt-stratified Antarctic lake, measuring approximately $5 \text{ km} \times 1 \text{ km} \times 50 \text{ m}$ deep. Their model was in good agreement with data obtained from the lake. We consider that this type of structure will also develop in magmas where the ratio of diffusivity of mass to that of heat is typically $< 10^{-5}$.

In this paper we obtain an expression for the temperature and cooling rate of the two layers as a function of time by using the quantitative relationships obtained from the study of a heat/salt system, allowing for the latent heat release due to crystallization and showing that the heat loss to the country rock can be neglected. Crystallization can occur on the floor of the chamber or within the convecting lower layer. For the latter case, the concentration of crystals with depth in the lower layer is obtained by comparing their (low Reynolds number) free-fall speed in a quiescent liquid with the root-mean-squared vertical turbulent velocity in a single convection layer. Initially the free-fall speed is small and crystals are held up by the convective motion, and are uniformly distributed with depth. With time, the crystal size increases, as does the fall speed, while the vertical convective velocity decreases due to the decreasing temperature difference between the two layers. The crystals begin to settle, leading to a concentration which increases towards the bottom. The quantitative analysis of these effects is presented and the results are applied to the case of picritic basalt and basalt magmas in subsequent sections.

Quantitative Analysis

The new magma ponds at the base of the chamber, because it is heavier than the resident magma, and cools by turbulent convection, because it is at a higher temperature. In order to quantify the thermal evolution of the lower layer, we apply standard relationships obtained for the analogous system of a layer of hot, salty water cooling under a layer of colder, fresher water. We expect that in this situation the two fluids – magma and brine – behave similarly and believe that it is scientifically desirable to evaluate quantitative predictions for our model which can be compared with field observations.

The compositional contribution due to MgO in the two layers, denoted by S and expressed as a weight fraction of the magma, is identified with the salt in the salt-water analogy. The turbulent heat flux is quantified according to the relationship (2.1) suggested by dimensional analysis, the background to which is explained by Turner (1979, p.274). The latent heat release accompanying the formation of olivine crystals is taken into account in the heat budget of the lower layer.

The quantitative results are first developed in generality and the specific values are inserted for the physical parameters.

(a) The Temperature History

The heat flux per unit area, F_H , through an interface between two fluids across which there is a temperature difference $\Delta T = T_1 - T_2$ and a compositional difference $\Delta S = S_2 - S_1$ as depicted in Fig. 1 can be shown, as argued extensively by Turner (1979, p.274), to take the form

$$F_H = \rho_0 c_p (g k_T^2 \alpha / \nu)^{1/3} \varphi(\beta \Delta S / \alpha \Delta T, \sigma, \tau) \Delta T^{4/3} \quad (1)$$

which incorporates the following physical properties in the layers: ρ_0 is the mean density, c_p is the specific heat, g is the acceleration due to gravity, k_T is the molecular diffusivity of heat, ν is the kinematic viscosity, α is the coefficient of thermal expansion, β is the proportional density change due to unit compositional change, the Prandtl number $\sigma = \nu / k_T$, $\tau = k_s / k_T$ with k_s equal to the molecular compositional diffusivity and φ is a non-dimensional function of three arguments. Experiments in which the compositional differences are due to salt ($\sigma \approx 10$, $\tau \approx 10^{-2}$) indicate that the function φ can be expressed as (Huppert 1971):

$$\varphi(\beta \Delta S / \alpha \Delta T; \sigma, \tau) = 0.32 (\beta \Delta S / \alpha \Delta T)^{-2}. \quad (2)$$

Substituting (2) into (1), we obtain

$$F_H = 0.32 \rho_0 c_p \alpha^2 (g k_T^2 \alpha / \nu)^{1/3} \beta^{-2} \Delta T^{10/3} \Delta S^{-2} \quad (3a)$$

$$\equiv \rho_0 c_p q \Delta T^{10/3} \Delta S^{-2} \quad (3b)$$

where (3b) is a definition of q . Since heat transfer rates are insensitive to the exact value of σ for σ larger than about 10 (Busse 1978), and are independent of τ for sufficiently small values which is the case for the magma considered here, we use (3) in quantifying the heat flux in our model. This may upset the quantitative accuracy of our predictions, especially for large $\beta \Delta S / \alpha \Delta T$ which is beyond the range yet achieved by laboratory experiments. We consider, however, that the qualitative descriptions of the cooling history of the system are correct.

The corresponding compositional flux, F_s is given in general terms by (Turner 1979)

$$F_s = (\alpha / \beta) \psi(\beta \Delta S / \alpha \Delta T; \sigma, \tau) (F_H / \rho_0 c_p) \quad (4)$$

where ψ is another function of three arguments. All experiments conducted so far, and all associated theory, suggest that for a wide range of $\beta \Delta S / \alpha \Delta T$, $\psi = \tau^{1/2}$ and is independent of σ so that (4) can be expressed as

$$F_s = (\alpha / \beta) \tau^{1/2} (F_H / \rho_0 c_p). \quad (5)$$

The fractional crystal content of the lower layer, x , is a function solely of T_1 , say $x = f(T_1)$. Considering the latent heat release due to crystallization (L cal gm^{-1}) in the heat budget for the two layers and using (5) and (3), we obtain

$$h_1 [1 - L c_p^{-1} f'(T_1)] \dot{T}_1 = -q (T_1 - T_2)^{10/3} (S_1 - S_2)^{-2} - (F_b / \rho_0 c_p) \quad (6a)$$

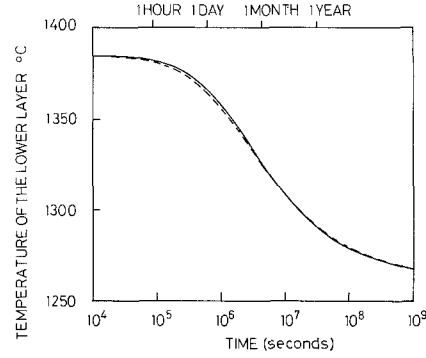


Fig. 2. Temperature of the lower layer as a function of time (t) for $\mu = 30$ poise, a compositional density difference $\rho_0 \beta \Delta S = 0.02$, an upper layer thickness $h_2 = 4$ km and a lower layer thickness $h_1 = 100$ m. The solid curve is the analytical result (11a), the dashed curve is the result of a numerical integration of (6)

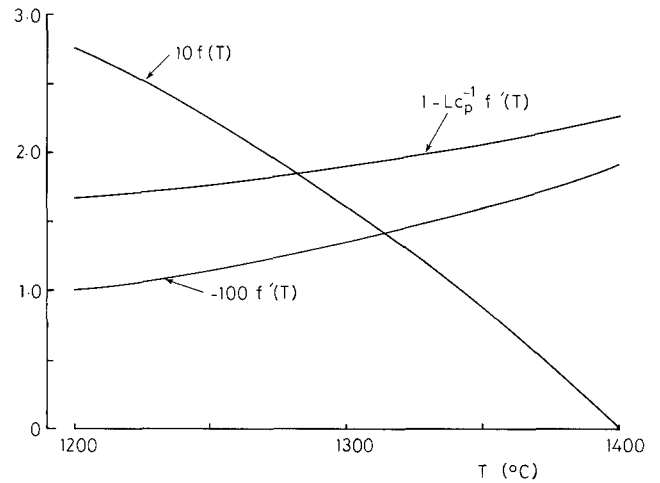


Fig. 3. Graphs of: $f(T) = (1,400 - T) / (1,924 - T)$; $f'(T)$; and $1 - L c_p^{-1} f'(T)$ with $L = 200$ cal gm^{-1} and $c_p = 0.3$ cal gm^{-1}

$$h_2 \dot{T}_2 = q (T_1 - T_2)^{10/3} (S_1 - S_2)^{-2} \quad (6b)$$

$$S_1 = (\alpha / \beta) q \tau^{1/2} (T_1 - T_2)^{10/3} (S_1 - S_2)^{-2} \quad (6c)$$

$$\dot{S}_2 = (\alpha / \beta) \tau^{1/2} \dot{T}_2 \quad (6d)$$

where F_b is the heat flux lost from the lower layer to the adjacent country rock. Before continuing we invoke the following simplifications. Since $(\alpha / \beta) \tau^{1/2}$ is typically very small ($\sim 5 \times 10^{-5}$), the compositional change due to transfer across the interface can be neglected and S_1 and S_2 set constant in (6). We show in the appendix that the conductive heat loss to the country rock is small compared to the convective term in (2.6a) and can be neglected. The remaining equations can be solved numerically, and the results of such a procedure are presented in Fig. 2.

Figure 3 presents a graph of $1 - L c_p^{-1} f'(T)$ for $f(T) = (1,400 - T) / (1,924 - T)$. In the case of olivine, the best available estimate of L is 200 cal gm^{-1} (Bottinga and Richet 1978), and $c_p = 0.3$ cal $\text{gm}^{-1} \text{C}^{-1}$. The expression for $f(T)$ is empirical, derived from the liquidus relationships found experimentally for picritic basalts in the range of MgO content 9 to 18% by Krishnamurthy and Cox (1977). The value of $1 - L c_p^{-1} f'(T)$ in Fig. 3 differs little from 2.0 which suggests inserting this value into the left-hand side of (6a).

This approximation allows the equations to be solved analytically and the dependence of the solution on the physical parameters to be easily assessed.

With these simplifications (6) become

$$\dot{T}_1 = -\frac{1}{2}A(T_1 - T_2)^{1/3} \quad (7a)$$

$$\dot{T}_2 = rA(T_1 - T_2)^{1/3} \quad (7b)$$

where

$$r = h_1/h_2 \quad (8)$$

and

$$A = q/(h_1 \Delta S^2) = 0.32(\alpha/\beta)^2 (g k_T^2 \alpha/\nu)^{1/3} / (h_1 \Delta S)^2. \quad (9)$$

The solution to (7) is determined by subtracting (7b) from (7a) solving the resulting equation for $T_1 - T_2$ and then using (7) to obtain

$$\dot{T}_1 = -\frac{1}{2}A[\Delta_0^{-7/3} + \frac{7}{3}A(r + \frac{1}{2})t]^{-1/7}. \quad (10)$$

Integration of (10) and (7b) leads to

$$T_1(t) = T_1(0) + \{[\Delta_0^{-7/3} + \frac{7}{3}A(r + \frac{1}{2})t]^{-3/7} - \Delta_0\} / (1 + 2r) \quad (11a)$$

$$T_2(t) = T_2(0) - 2r \{[\Delta_0^{-7/3} + \frac{7}{3}A(r + \frac{1}{2})t]^{-3/7} - \Delta_0\} / (1 + 2r) \quad (11b)$$

where Δ_0 is the initial temperature difference between the layers. $T_1(t)$, as given by (11a), is plotted as the solid curve in Fig. 2. The difference between this curve and the more accurate, numerically obtained solution, represented by the dashed curve, is insignificant; henceforth the discussion will use the analytical relationships (10) and (11).

(b) The Interface Thickness

The thickness of the thermal interface between the two layers can be evaluated by using the fact that the heat transfer between the layers is by molecular diffusion. Hence the thickness, say d , is given by

$$F_H = \rho_0 c_p k_T \Delta T / d. \quad (12)$$

Representing F_H by (3b) and using the definition of A given in (9), we can thus write

$$d = (k/Ah_1) \Delta T^{-7/3}. \quad (13)$$

Table 1 presents values of d for a number of different values of ΔT . It can be seen that the interface thickness grows with time as the temperature difference decreases. It should be borne in mind that the interface will not remain perfectly horizontal, but will oscillate somewhat in position in response to the buffeting it receives from the turbulent eddies in both layers.

(c) Crystallization and Crystal Settling

Cooling of the lower layer results in crystallization. Two circumstances of crystallization can be envisaged. The first situation is when crystallization occurs on the floor of the chamber and the

Table 1. The thickness of the interface between the layers for various temperature differences, as given by (13) with $Ah_1 = 8.3 \times 10^{-10} \text{ ms}^{-1} (\text{C}^\circ)^{-1/3}$

ΔT (C°)	130	100	50	25	10
d (m)	0.01	0.02	0.10	0.52	4.7

second situation is when crystals are precipitated throughout the liquid. We now consider in detail the second circumstance.

The study of the behaviour of small particles in a turbulent medium is still in its infancy, despite numerous important applications such as sand in rivers, aerosols in air and crystals in magma chambers. Batchelor (1965) argues that a steady-state distribution of small but heavy particles in a fluid results from the balance between the downward flux of particles due to gravity and upward flux due to turbulent exchange processes. The downward concentration flux per unit horizontal area can be estimated as VC where V is the terminal velocity of a particle in the absence of any turbulence and C is the concentration which will be a slowly varying function of height. The upward turbulent transport flux can be written as $-e dC/dy$ where e is the eddy diffusivity and y the vertical co-ordinate. Since the turbulent convective eddies will extend throughout the lower layer, $e \sim wh$, where w is the root-mean-square vertical velocity. Thus the steady-state concentration of particles is given by

$$VC = -wh_1 \frac{dc}{dy} \quad (14)$$

the solution of which for constant w is

$$c = c_0 \exp[-Vy/(wh_1)] \quad (15)$$

where C_0 is the particle concentration at $y=0$. Thus if $V \ll w$, the concentration is almost uniform throughout the layer, while if $V \gg w$, the concentration at the top of the layer is exponentially small compared with that at the bottom: the particles have virtually settled.

In a one-component layer, with a Rayleigh number greater than about 10^7 , the convection is fully turbulent (Krishnamurthi 1970). Under this condition, similarity theory indicates that w_m , the maximum value of w is dependent only upon the heat flux and the depth of the layer. It can thus be expressed as

$$w_M = (\alpha g F_H h_1 / \rho_0 c_p)^{1/3}, \quad (16)$$

Experiments (Deardorff and Willis 1967) indicate that w increases monotonically from zero at the base of the layer to approximately w_m in the middle of the layer before returning to zero at the top of the layer (Townsend 1976, Fig. 8.13). Extending the above results to our two-component system, we write

$$w = (\alpha g A h_1^2)^{1/3} \Delta T^{1/9}, \quad (17)$$

The terminal velocity of an isolated spherical crystal is

$$V_1 = \frac{2}{9} a^2 g \Delta \rho / \nu \quad (18)$$

where a is the radius of the crystal and $\Delta \rho$ its density excess over the fluid in which it resides. For non-spherical crystals the multiplicative factor $2/9$ which appears in (18) must be altered by an amount which depends on the exact shape of the crystals. The effect of increasing crystal concentration on the settling velocity of individual spherical crystals can be estimated by (Barnes and Mizrahi 1973)

$$V/V_1 = (1-E) \exp[-\frac{5}{3}E(1-E)^{-1}] / (1+E^{1/3}) \quad (19)$$

where E is the volume fraction of crystals.

(d) Constraints on Parameters

Although the above analysis can be applied to any dense hot magma intruded into a reservoir of lighter magma, we concentrate in this paper on the case of picritic basalt melt intruded into a

Table 2. Chemical compositions of melts used in our illustrative models. Composition 1 is Elthon's estimates (1979) of the average composition of the oceanic crust. Compositions 2–5 are residual liquids derived by successive crystallisation of olivine (FO_{90}) from composition 1. Estimates of liquidus temperature, density and viscosity are listed for each melt. The amount of olivine required to generate the liquids 2–5 from composition 1 are also listed. ρ_b is the bulk density of the magma (crystals plus melt)

	1	2	3	4	5
SiO ₂	47.76	48.12	48.52	48.97	49.48
Al ₂ O ₃	12.06	12.69	13.40	14.19	15.08
FeO	8.96	8.91	8.87	8.82	8.77
MnO	0.12	0.12	0.13	0.13	0.14
MgO	17.78	16.11	14.27	12.21	9.88
CaO	11.20	11.79	12.44	13.18	14.00
Na ₂ O	1.31	1.38	1.45	1.54	1.64
K ₂ O	0.03	0.03	0.03	0.03	0.03
TiO ₂	0.59	0.62	0.66	0.69	0.72
Temp. (°C)	1,385	1,360	1,325	1,290	1,255
ρ (gm/cm ³)	2.723	2.717	2.711	2.705	2.700
ρ_b	2.723	2.746	2.770	2.795	2.820
μ (poise)	8.83	13.65	22.31	46.33	100.5
Crystal content		5%	10%	15%	20%

basaltic magma chamber. There is a large amount of petrological literature, some referred to earlier, which points to this situation being important, in the evolution of associated basic and ultrabasic igneous rocks.

Table 2 shows the composition (no. 1) of a representative picritic basalt magma. Elthon (1979) estimated this composition as a suitable parent for tholeiitic basalts in the ocean crust from the relative abundance of rock types in ophiolite complexes. There is a growing consensus amongst petrologists, based on a wide variety of experimental and geochemical studies, that the parental magmas to many tholeiitic basalt suites have MgO content of between 15% and 20% and are, in broad terms, compositionally similar to Elthon's estimate (see for example O'Hara 1968; Irvine 1979; Green et al. 1979; Clarke and O'Hara 1979; Berg 1980; and Smewing 1980). Compositions 2–5 are successive liquids produced by crystallization of olivine (FO_{90}) from a melt of composition 1. Liquidus temperatures are estimated from the experimental determinations at a pressure of one atmosphere of a similar picritic basalt by Krishnamurthy and Cox (1977). Thompson (1973) has shown that there is an approximately linear relationship between MgO content (MgO > 10%) of a basaltic melt and liquidus temperature.

Table 2 also shows the variation of melt density and viscosity and the bulk magma density (crystals plus melt) with composition for the case where crystals are precipitated throughout the lower layer. In Eq. (7) it is analytically sufficient to take viscosity as constant (30 poise) because the parameter A is weakly dependent on viscosity. The settling velocity of olivine crystals is strongly dependent on viscosity [Eq. (18)] and the precise values of melt viscosity are used in calculating settling velocities. We assume that the picritic basalt has no yield strength while olivine is the only major liquidus phase and have calculated the liquid viscosities by the method of Shaw (1972). Magmas can become non-Newtonian when plagioclase joins as a crystallizing phase (McBirney and Noyes 1979), considerably complicating rheological behaviour.

Densities are calculated by the method of Bottinga and Weill (1970) using values of partial molar volumes presented by Nelson and Carmichael (1979). Figure 4 shows a plot of melt density

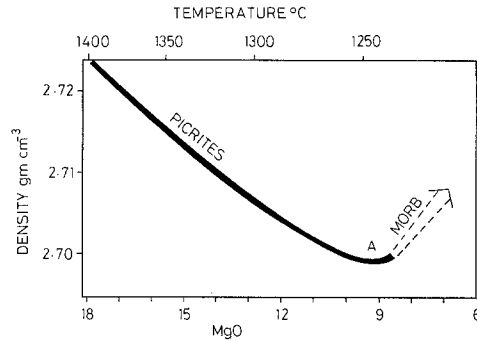


Fig. 4. Variation of melt density with MgO content in picrite liquids. The estimate of Elthon (1979) for the parental magma to the ocean crust with MgO ~ 17.8% was taken as a starting point and a succession of liquid comparisons down to MgO = 10% generated by the removal of forsterite (FO_{90}). Liquidus temperatures were estimated from the experimental data of Krishnamurthy and Cox (1977). The density minimum at A is illustrated with the approximate trend of MOR basalt density with MgO content for MgO less than 9% (Sparks et al. 1980)

Table 3. The values of 5 parameters used in the calculations

$\alpha = 5 \times 10^{-5} \text{ K}^{-1}$
$\kappa = 8 \times 10^{-7} \text{ m}^2 \text{ s}^{-1}$
$\nu = 10^{-3} \text{ m}^2 \text{ s}^{-1}$
$\sigma = 2 \times 10^{-2}$
$\tau \sim 10^{-3}$

against MgO content, which illustrates a characteristic feature of the low-pressure evolution from picritic magma to tholeiitic basalt. When olivine is the only major fractionating phase, magma melt density decreases (Sparks et al. 1980; Stolper and Walker 1980). This decrease continues until the melt reaches a cotectic boundary at which plagioclase, and perhaps pyroxene, join olivine as the crystallizing phase. Plagioclase crystallization generally causes melt density to increase as discussed by Sparks et al. (1980).

A marked density minimum is thus attained during the evolution of tholeiitic magmas. Compositions which occupy this density minimum typically contain 9–11% MgO. Glasses with such compositions are amongst the most primitive to be recovered from mid-ocean ridges and to be found as aphyric lavas in ophiolite complexes. In several layered igneous complexes the 'parental' basaltic magmas also have composition which fall in this minimum (generally with high CaO and Al₂O₃ contents). For our calculations the resident magma is assumed to have the composition of analysis 5 (Table 2).

Other physical properties required are listed in Table 3. The value of latent heat of crystallization of olivine ($L = 200 \text{ cal gm}^{-1}$) is taken from Bottinga and Richet (1978). A value of $L = 100 \text{ cal gm}^{-1}$ is often taken for basalt solidification, but Bottinga and Richet (1978) document a considerable range in L values for the common basic minerals from over 200 cal gm⁻¹ (forsterite) to 50 cal gm⁻¹ (albite).

In the case of the water/salt system the parameter ΔS represents the difference in salinity between the two layers. In the case of magma, the definition of ΔS is related to several components causing differences in melt density. For the picritic basalt system, considered in detail below, the essential difference in composition is the normative olivine content for magnesian-rich compositions. Olivine component plays an analogous role to salinity in the magma. The parameter $\rho_0 \beta \Delta S$ thus expresses the density contrast between the two layers due to compositional effects.

The dimensions of basaltic magma reservoirs have been estimated by a variety of indirect methods. Seismic studies of mid-ocean ridges (Rosendahl 1976; Nisbet and Fowler 1978) and of basaltic central volcanoes (Bjornsson et al. 1979) provide evidence of high-level magma storage, but only allow qualitative inferences to be made concerning the shape and dimensions of the reservoirs. Lava flows from central volcanoes in Iceland have volumes of several km³ (Sigurdsson and Sparks 1978). Many such lavas have been extensively fractionated at low pressure, implying substantial storage chambers. The dimensions of magma chambers can also be estimated from the lateral extent and composition of layers in cumulate sequences. Smewing (1980), for example, has deduced that the magma chambers beneath the spreading centre that formed the North Oman ophiolite reached 10 km in one horizontal dimension with vertical heights up to 3.5 km. In view of such studies we adopt thicknesses in the range of 0.5 m to 5 km for the value of h_2 and 3 to 500 m for the value of h_1 (Fig. 1b).

Finally, olivine crystal dimensions in ultrabasic cumulates and in olivine phyric lavas are typically in the range 0.1 to 0.5 cm.

Results

(a) Cooling Rates

Figure 5 shows the variation of initial cooling rates of the lower layer, $\dot{T}_1 = \frac{1}{2} A \Delta_0^{1/3}$, as a function of Δ_0 and h_1 . The initial cooling rates were calculated with a

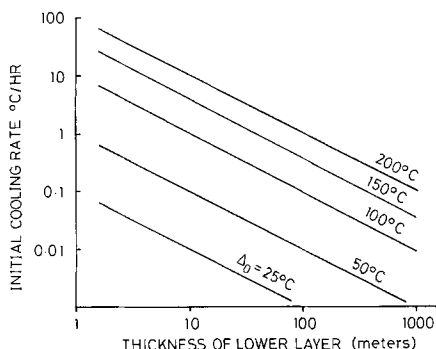


Fig. 5. Initial cooling rate of the lower layer as a function of the lower layer thickness (h_1) and the initial temperature contrast (Δ_0) for $\mu = 10$ poise and compositional density difference $\rho_0 \beta \Delta S = 0.02$

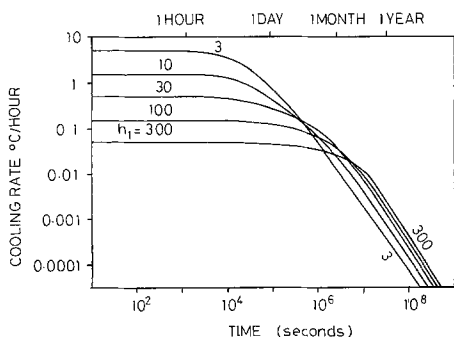


Fig. 6. Cooling rate of the lower layer as a function of time (t) and lower layer thickness (h_1) for $\mu = 30$ poise, a compositional difference $\rho_0 \beta \Delta S = 0.02 \text{ gm cm}^{-3}$ and upper layer thickness $h_2 = 4 \text{ km}$

viscosity of 10 poise, appropriate to the initial temperature of a picritic basalt layer. In all other calculations on the subsequent history of the layer a mean value of 30 poise was used. Figure 6 shows the variation of cooling rate with time as given by (10) for $h_2 = 4 \text{ km}$ and $\Delta_0 = 130^\circ \text{C}$ for a range of values of h_1 (3 to 300 m). These results are relevant to the case where a melt of composition 1 (Table 2) forms the lower layer and a melt of composition 5 forms the upper layer. Both Figs. 5 and 6 show that if the temperature difference is large (100° to 200°C), or the layer thickness is thin (of the order of a few metres), rapid cooling rates can occur.

Figure 6 also illustrates a striking division of the cooling history of the lower layer into a period of rapid cooling rates followed by a long period of steady decline in cooling rate. The initial period in fact produces most of the temperature decline in the lower layer.

(b) Temperature Variations

Figure 7a shows the temperature of the lower layer as a function of time for $h_2 = 4 \text{ km}$ and various h_1 (3

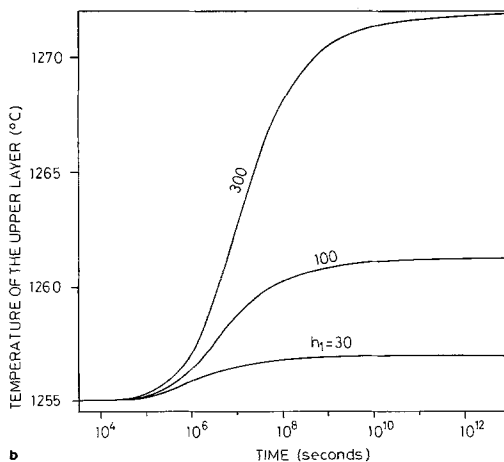
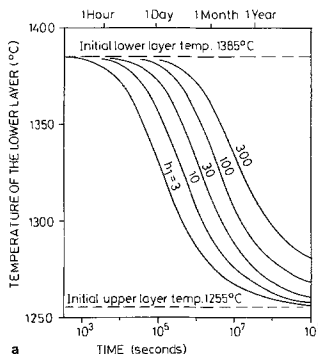


Fig. 7. **a** Temperature of the lower layer as a function of time (t) and lower layer thickness (h_1) for $\mu = 30$ poise, a compositional density difference $\rho_0 \beta \Delta S = 0.02 \text{ gm cm}^{-3}$ and upper layer thickness $h_2 = 4 \text{ km}$. **b** Temperature of the upper layer as a function of time (t) for the same conditions as used in (a)

to 300 m), $\Delta_0 = 130^\circ\text{C}$ and a mean viscosity of 30 poise. For these conditions we observe that most of the temperature decline takes place within periods of a few weeks to a few years. Alteration of the principal parameters (Table 2) within plausible limits for basaltic and picritic basalt magmas and for different chamber dimensions would not significantly alter this conclusion. In comparison to the total cooling time of basaltic magma chambers by conductive cooling to country rocks (Usselman and Hodge 1978), which may take tens of thousands of years, the lower layer equilibrates thermally with the more voluminous upper layer exceedingly quickly.

Figure 7b shows the temperature of the upper layer for the same conditions as used in preparing Fig. 7a. The temperature increase in the upper layer has a number of petrological consequences outlined below.

(c) Turbulent Velocities

Figure 8a shows the variation of the characteristic turbulent eddy velocity computed from (17) as a function of time for the same conditions as used for Fig. 7a.

The settling velocities of olivine crystals with density excess of 0.6 gm cm^{-3} and with diameters ranging from 0.2 to 1.0 cm diameter in a fluid with viscosity of 100 poise, are also shown. Clearly in all circumstances the initial convective velocities far exceed the settling velocities of the olivine phenocrysts typically observed in ultrabasic rocks. The velocities of the crystals only become comparable to the turbulent velocities when the temperatures of the two layers are very close.

Figure 8b shows the decline of w_m with time for a 10 m thick layer under the same conditions as Fig. 7. The figure also shows the settling velocities of olivine crystals with time in the lower layer. The settling velocities decrease as the melt viscosity increases and the concentration of olivines increases. Again for a long time after the rapid cooling phase has ended, the turbulent velocities of the lower layer greatly exceed, by over an order of magnitude, the settling velocities of the olivines. We predict a nearly uniform distribution of olivines suspended in the lower layer until a late stage in its cooling history.

One consequence of the decrease in turbulent velocities toward the boundary of a convecting layer is relevant to the sedimentation of crystals. From Eq. (17) it is evident that turbulence will decay close to the chamber floor and that even during the early stages of cooling, a crystal that reaches close enough to the base of the layer can settle. The boundary layer in which sedimentation can occur will increase in thickness with time. Thus sedimentation will become

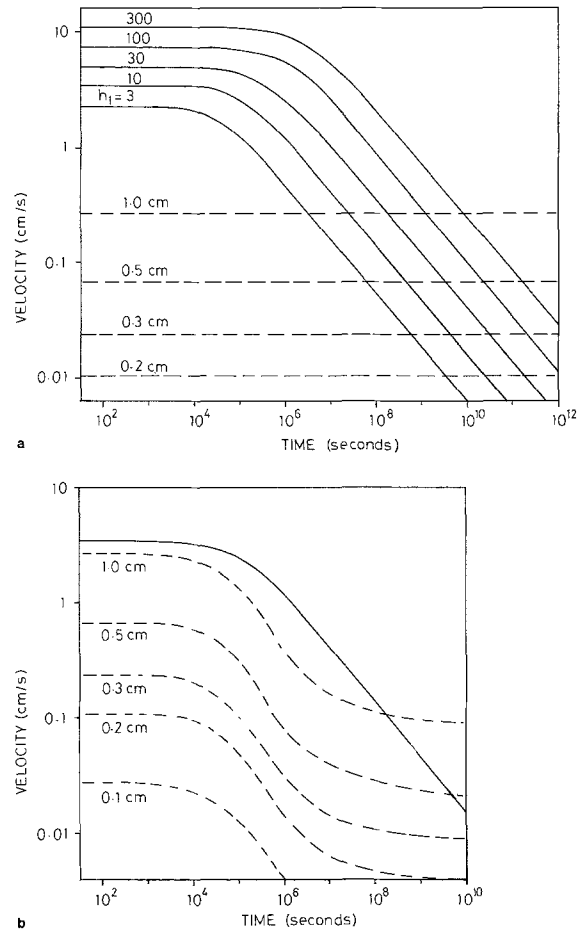


Fig. 8. a Mean turbulent vertical velocity in the lower layer, given by (17), as a function of time (t) and lower layer thickness (h_1) for the same conditions as used in Fig. 7. The dashed lines indicate the settling velocities of olivine crystals with a density excess of 0.6 gm cm^{-3} as a function of their diameter (in cm) in a fluid with $\mu = 100$ poise. b The mean turbulent settling velocity for $h_1 = 10\text{ m}$ is shown by the solid line for the same conditions as (a). The light dashed lines are the settling velocities of olivine crystals as a function of time. Each curve shows the settling velocities of a crystal of constant diameter. The settling velocities vary with time due to the increasing melt viscosity and crystal concentration

progressively more important as the lower layer cools.

We conclude this section with comments on two parameters implicit in the model. First, the Rayleigh number of the lower layer, typically exceeds 10^9 , thus justifying the assumption that it is turbulent. Second, the Reynolds number of the crystals which is at most 10^{-2} , thus justifying the use of the Stokes free-fall relationship (18).

Some Geological Applications

Cyclic Layering in Ultrabasic Rocks

Large-scale cyclic layering is a common feature in the ultrabasic parts of intrusions. In such a sequence of

layered rocks each unit shows part or all of a progression from one end member of a suite to the other (Brown 1956; Smewing 1980). The path of fractional crystallization is usually represented in each unit with a typical change from ultramafic to mafic layers. Cyclic units are generally interpreted as the result of periodic replenishment of a magma body by primitive magma (Brown 1956; Irvine and Smith 1967; Smewing 1980). We propose that these cyclic units are the consequence of the formation of two layers in a magma chamber as outlined in our model and shown in Fig. 1. We now interpret the principal features of cyclic units in terms of our quantitative fluid dynamic model.

A well-documented example is the Rhum ultrabasic intrusive complex, NW Scotland, where over fifteen cyclic units were identified by Brown (1956). Each unit consists of a lower peridotite layer (olivine cumulate) and an upper leucocratic layer (plagioclase-pyroxene-olivine cumulate). The cyclic units vary from about 15 to 175 m and average 60–70 m in thickness with the peridotite layer usually being the thicker part. The layers extend laterally up to 5 km. A thin chromitite seam often occurs at the base. Detailed sections through individual units (Brown 1956; Maaloe 1978; Dunham and Wadsworth 1978) show that the peridotite layer is remarkably homogeneous with no cryptic variation, no obvious crystal sorting (typical dimension 0.1 cm) and little modal variation. The transition to the upper leucocratic cumulates is fairly abrupt (a few metres) and the upper layer shows marked rhythmic layering and cryptic variation.

The replenishment model of Brown (1956) has generally been accepted by later workers, though the nature of the influxing magma has been debated: Brown (1956) and Dunham and Wadsworth (1978) favour a basaltic magma, whereas Gibb (1976) suggests a basaltic liquid rich in suspended olivine phenocrysts (ultrabasic bulk composition).

We now suggest a modification of the replenishment model and interpret each cycle as the consequence of influx of picritic basalt magma. The composition of the reservoir magma is taken as similar to that proposed by Brown (1956) with $\text{MgO} \sim 10\%$ and the picritic basalt magma is taken as much more magnesian rich ($\text{MgO} \sim 20\%$) following Gibb (1976). In terms of MgO content, temperature and density such magmas would be comparable to compositions 1 and 5 (Table 2) which we used before in our illustrative calculations. The denser picritic basalt spreads over the chamber floor forming a layer a few tens of metres thick. Room is made for the new liquid either by eruption (Brown 1956) subsidence, or by injection of dykes. The lower

picritic basalt layer cools rapidly as previously described and olivine precipitates, but remains suspended due to the vigorous convection. Chromite seams, observed at the base of some Rhum cyclic units, can be formed by hybridisation between the new magma, the resident magma and melted chamber floor by the mechanism proposed by Irvine (1977). Some resident magma is inevitably trapped as the picritic basalt spreads out over the chamber floor and the plagioclase-rich floor is likely to melt providing the opportunity for contamination.

The two layers convect vigorously as they exchange heat. If the typical influx of new magma associated with the formation of a Rhum cyclic unit represents approximately 10% of the chamber volume, as envisaged by Brown (1956), then a substantial part of the heat exchange will be accomplished in a few years (Fig. 5). The lower layer will evolve into a dispersion of olivine crystals in a basaltic liquid. As convection dies down in the lower layer, settling of olivine crystals begins and becomes increasingly important. Little sorting can occur during *en masse* olivine sedimentation and a thick layer of olivine crystals of relatively uniform size will form (the peridotite layer). The olivines would be of uniform composition having grown in a well-mixed convecting layer.

As the olivines sediment, residual basaltic liquid remains in the lower layer. However, for values of the ratio $h_2 : h_1$ of about 10, the residual liquid will have a composition close to the density maximum (Fig. 4) and therefore would mix convectively with the overlying basalt layer. The upper layer, now a hybrid of pre-existing basaltic magma and the residual basalt magma from the lower layer, returns to the generation of plagioclase-pyroxene-olivine cumulates until interrupted by the influx of new magma.

The same model can be applied to cyclic units found at the base of ophiolite complexes. A particularly well-documented succession has been described by Smewing (1980) from the ophiolite of North Oman, who proposes a similar model to that advanced here. Each cyclic unit consists of dunite or peridotite, ranging in thickness from a few metres to several hundred metres, overlain by olivine gabbro. The transition from ultramafic to mafic cumulates in each unit is abrupt, marked by changes in mineral compositions and proportions.

Smewing interprets each cyclic unit as evidence of the influx of picritic basalt magma into a large chamber beneath a fast-spreading ridge. In many cases, the olivine compositions of the ultramafic parts of each unit are much more primitive (fosteritic) than the olivines in the underlying gabbro of the previous unit. He concludes from these observations that the new

influx of primitive magma does not immediately mix throughout the chamber, but undergoes a period of crystallization as an independent layer. During this period, the ultramafic part of the bimodal unit is formed. The abrupt transition to gabbros represents, according to Smewing, eventual mixing of the new magma with the much larger volume of fractionated basalt in the chamber.

We agree with Smewing's interpretation and suggest that the same model outlined for the Rhum layers can be applied to the Oman rocks. In Oman the primitive magma MgO content is also estimated as about 18%. For one peridotite unit 50 m thick, which precipitated Fo_{91} olivine Smewing estimates that the body of liquid from which the layer formed was four times the volume of the layer. He also estimates the chamber height as being of the order of 3.5 km. The lavas in this ophiolite are typical mid-ocean ridge tholeiites ($\text{MgO} < 10\%$). If these figures are accepted then, with a value of the ratio $h_2 : h_1$ of between 10 and 20, and similar magmas involved to those compositions in Table 2, the results of our quantitative calculations are directly applicable. As outlined by Huppert and Sparks (1980), a large magma chamber beneath an oceanic spreading centre will operate as a trap for magmas with $\text{MgO} > 10\%$. The Oman ophiolite is suggested as an example of a situation where the mechanism of layering has operated repeatedly and efficiently, producing compositional stratification in the ophiolitic oceanic crust and limiting the range of melts which can reach the surface.

Quench Textures in Layered Rocks

Donaldson (1976) has shown in experiments that olivine crystal morphology is related to the cooling rate and melt composition (particularly MgO content). Donaldson reproduced hollow hopper-shaped crystals at cooling rates of 2.5 to 15°C/h and elongate crystals at cooling rates of 15° to 40°C/h. Both these morphological varieties occur in ultrabasic cumulates. For example, on Rhum spectacular comb-layering (harrisite) is apparently the result of large branching olivine crystals growing vertically from the chamber floor. There are many possible ways of forming comb-layering (Donaldson 1977). Conditions for generating rapid cooling (Fig. 5) that are appropriate for forming such layering in ultrabasic intrusions could occur when thin layers of hot ultrabasic magma spread out over the base of a basaltic magma chamber.

Donaldson (1977) has also suggested that the layering was formed during relatively quiescent periods in the magma chamber. It is worthwhile pointing

out that the thin layers show the least vigorous convection (Fig. 8) because of their relatively smaller Rayleigh number. Thus thin layers are predicted to show a combination of rapid cooling rates and relatively low degrees of turbulence. Comb-layering can also be observed on the vertical walls of magma chambers (Wager and Deer 1939), which cannot be attributed to the process suggested here.

Evidence for the formation of quench textures in layered igneous intrusions during the influx of ultrabasic magma to a basaltic chamber has recently emerged from the study of the Hettash Intrusion, Labrador (Berg 1980). Berg provides evidence for the influx of an ultrabasic magma ($\text{MgO} \sim 19.3\%$) into a magma chamber containing alumina-rich basalt ($\text{MgO} \sim 7.6\%$). A highly distinctive troctolitic horizon can be traced over 17 km with a thickness of a few metres. This layer contains much more calcic plagioclase and forsteritic olivine than the anorthositic cumulates both above and beneath. The layer also displays spectacular comb-layering of plagioclase and snowflake texture (largescale spherulitic plagioclase). Berg interprets the layer as due to the spreading of an ultrabasic melt over the floor of the chamber and its rapid cooling. Our model supports this interpretation and predicts suitably high cooling rates for a 10 m thick layer (Figure 5).

Conclusions and Discussions

A general model has been presented for the intrusion of a hot and dense magma into the base of a magma reservoir. In this circumstance, two layers are formed which turbulently convect and exchange heat across a stable interface. There is no extensive mixing of the new magma with the resident magma. The detailed structure of interface is controlled by the lower diffusivity of chemical components in the two magmas in comparison to the diffusivity of heat.

Equations (10) and (11) allow the cooling rate and temperature of each layer to be predicted as a function of time. The cooling history is controlled by the physical properties of the magmas and the relative thicknesses of the two layers. In the case of the ultrabasic and basic magmas, cooling times are of the order of a few months to a few years, illustrating the rapid rates of heat transfer in this situation. The lower layer cools to equilibrium with the upper layer, but remains at virtually the same composition as it had originally.

In this paper we have emphasised the case where crystallization occurs within the convecting liquid. An important result of the calculations is that convective velocities are too rapid to allow crystals to settle during cooling. However, crystal settling occurs

at a late stage of the evolution, when the system is close to thermal equilibrium. The growth of suspended olivine in the lower layer could lead to a situation of equilibrium crystallization and little or no compositional variation in the resulting cumulate layer. There may, however, be circumstances where crystallization takes place on the chamber floor. In such case progressive removal of olivine at the base of base of the cooling lower layer would lead to a situation of fractional crystallization.

In either case, the model provides an explanation for the formation of bimodal cyclic units in layered intrusions. Ultrabasic magma is intruded into a basaltic reservoir, forms a separate layer and undergoes a period of independent crystallization. Eventually the residual liquid becomes buoyant and mixes with the overlying basalt. The residual liquid is likely, in many plausible circumstances, to be close to the density minimum with MgO 9–11%. The model thus suggests reasons for the restrictions in the compositions of erupted tholeiitic basalt liquids in an open-system magma chamber.

We are aware that more complex crystallization sequences can be envisaged than that treated here in associated basic and ultrabasic magmas, depending on pressure, temperature, volatile content and bulk magma compositions. Thus, for example, some ultrabasic magmas can evidently precipitate highly calcic plagioclase (Berg 1980). We can also envisage situations where, after sedimentation of olivine, the residual magma is still denser than the overlying layer. Other types of cumulate could then form, such as werhlite or pyroxenite, before the residual magma in the lower layer becomes sufficiently light to mix with the overlying magma layer. These other circumstances may involve slight modification of the assumptions we have made on the relationship of composition to the relevant physical properties. However, these modifications will not affect the broad conclusions of the model, which apply to a wide range of possible situations, for which the fundamental assumptions of relevant densities and temperatures are upheld.

There are other magmatic associations which could be considered in the light of such a model. Analogous behaviour can be anticipated in, for example, various members of the basalt-andesite-dacite group. In this association liquid density decreases progressively with crystallization and repeated injection of dense basic magma could lead to the formation of a chemically-zoned magma chamber. We have only given detailed attention here to a few specific cases of basic and ultrabasic rock associates to illustrate the potential of the model for interpreting igneous rocks.

Acknowledgements. Helpful comments from C.H. Donaldson, D.P. MacKenzie, and J. Stewart Turner are much appreciated. Department of Earth Sciences Contribution No. 52, University of Cambridge.

Appendix

The purpose of this appendix is to demonstrate that the conductive heat loss to the country rock at the base of the chamber can be neglected in the calculation of the temperature history of the lower layer.

The effect of the relatively cold country rock is to cool the bottom of the lower layer and quench the convection at the base of the layer. Thus the heat transfer from the lower layer to the country rock is by conduction. This situation may be modelled by a semi-infinite region in $y < 0$ (the country rock), initially at a temperature of $T_c(0)$, below a semi-infinite region, initially at $T_1(0)$. The temperature profile in the upper region is then (Carslaw and Jaeger, 1959, p. 88).

$$T_1(t) = T_c(0) + [T_1(0) - T_c(0)] \left\{ K_1 k_1^{-1/2} + K_c k_c^{-1/2} \operatorname{erf} \left[\frac{1}{2} y / (k_1 t)^{1/2} \right] \right\} / (K_1 k_1^{-1/2} + K_c k_c^{-1/2}), \quad (\text{A1})$$

where K is the thermal conductivity and subscripts 1 and c refer to the upper and lower regions respectively. For $y / (k_1 t)^{1/2} \gg 1$ the temperature in the upper region is $T_1(0)$, and the flux of heat at the base of the upper region is

$$\rho_0 c_p [\pi^{-1/2} K_c (k_1/k_c)^{1/2} / (K_1 k_1^{-1/2} + K_c k_c^{-1/2})] \cdot [T_1(0) - T_c(0)] t^{-1/2}.$$

Provided $h_1 / (k_1 t)^{1/2} \gg 1$, we can use the results of this model to estimate the heat flux from the lower layer of the magma chamber to the country rock by writing

$$F_B / \rho_0 c_p = [\pi^{-1/2} K_c (k_1/k_2)^{1/2} / (K_1 k_1^{-1/2} + K_c k_c^{-1/2})] \cdot [T_1(t) - T_c] t^{-1/2}, \quad (\text{A2})$$

where T_c is the far-field temperature of the country rock. Setting $K_1 = K_c$ and $k_1 = k_c = 10^{-2} \text{ cm}^2 \text{ s}^{-1}$ in (A2), inserting it into (2.6) and solving the equations numerically, we obtain results which cannot be distinguished from those obtained by setting $F_B = 0$. We conclude that the conductive heat flux from the base of the magma chamber can be neglected.

References

- Anderson AT (1976) Magma mixing: petrological process and volcanological tool. *J Vol Geoth Pres* 1:3–33
- Barnea E, Mizrahi J (1973) A generalized approach to the fluid dynamics of particulate systems. Part I. General correlation for fluidization and sedimentation in solid multiparticle systems. *Chem Eng* 5:171–189
- Batchelor GK (1965) The motion of small particles in turbulent flow. *The Second Australian Conference on Hydraulics and Fluid Mechanics* 019–041
- Berg JH Snowflake troctolite in the Hettasch Intrusion, Labrador: evidence for magma-mixing and supercooling in a plutonic environment. *Contrib Mineral Petrol* (in press)
- Bjornsson A, Johnsen G, Sigurdsson S, Thorbergsson G, Truggvason E (1979) Rifting of the plate boundary in North Iceland, 1975–1978. *J Geophys Res* 84:3029–3038
- Bottinga Y, Richet P (1978) Thermodynamics of liquid silicates. A preliminary report. *Earth Planet Sci Lett* 40:382–400

- Bottinga Y, Weill DF (1970) Densities of liquid silicate systems calculated from partial molar volumes of oxide components. *Am J Sci* 269:169-182
- Brown GM (1956) The layered ultrabasic rocks of Rhum Inner Hebrides. *Philos Trans R Soc London B*240:1-53
- Busse FH (1978) Non-linear properties of thermal convection. *Rep Prog Phys* 41:1929-1967
- Carslaw HS, Jaeger JC (1959) *Conduction of Heat in Solids*. Oxford University Press
- Clarke DB, O'Hara MJ (1979) Nickel and the existence of high magnesia liquids. *Earth Planet Sci Lett* 44:153-158
- Cox KG (1978) Komatiites and other high-magnesia lavas: some problems. *Philos Trans R Soc London A*288:599-509
- Deardorff JW, Willis GE (1967) Investigation of turbulent thermal convection between horizontal plates. *J Fluid Mech* 28:675-704
- Donaldson CH (1976) An experimental investigation of olivine morphology. *Contrib Mineral Petrol* 57:187-213
- Donaldson CH (1977) Laboratory duplication of comb-layering in the Rhum pluton. *Mineral Mag* 41:323-336
- Donaldson CH, Brown RW (1977) Refractory megacrysts and magnesium-rich melt inclusions with spinel in oceanic tholeiites: indicators of magma mixing and parental magma composition. *Earth Planet Sci Lett* 37:81-89
- Dunham AC, Wadsworth WJ (1978) Cryptic variation in the Rhum layered intrusion. *Mineral Mag* 42:347-356
- Eichelberger JC (1978) Andesitic volcanism and crustal evolution. *Nature* 275:21-27
- Elthon D (1979) High magnesia liquids as the parental magma for ocean floor basalts. *Nature* 278:514-518
- Gibb FGF (1976) Ultrabasic rocks of Rhum and Skye: the nature of the parent magma. *J Geol Soc, London* 132:209-222
- Green DH, Hibberson WO, Jacques AL (1979) Petrogenesis of mid-ocean ridge basalts. In: E McElhinny (ed), *The Earth: its origin, structure and evolution*, pp 265-289
- Hildreth WS (1979) The Bishop Tuff: Evidence for the origin of compositional zonation in silicic magma chambers. *Geol Soc Am, Spec Pap* 180:43-76
- Huppert HE (1971) On the stability of a series of double-diffusive layers. *Deep-Sea Res* 18:1005-1021
- Huppert HE, Sparks RSJ (1980) Restrictions on the compositions of mid-ocean ridge basalts: a fluid dynamical investigation. *Nature* 286:46-48
- Huppert HE, Turner JS (1972) Double-diffusive convection and its implications for the temperature and salinity structure of the ocean and Lake Vanda. *J Phys Oceanogr* 2:456-461
- Irvine TN (1977) Origin of chromitite layers in the Muskox intrusion and other stratiform intrusions: a new interpretation. *Geology* 5:273-277
- Irvine TN (1979) Rocks whose composition is determined by crystal accumulation and sorting. In: HS Yoder Jr (ed), *The Evolution of Igneous Rocks*, pp 245-306
- Irvine TN, Smith CH (1967) The ultramafic rocks of the Muskox Intrusion. In: PJ Wyllie (ed), *Ultramafic and Related Rocks*. John Wiley & Sons, New York, pp 38-49
- Krishnamurthy P, Cox KG (1977) Picrite basalts and related lavas from the Deccan Traps of Western India. *Contrib Mineral Petrol* 62:53-75
- Krishnamurthy R (1970) On the transition to turbulent convection. Part 2. The transition to time-dependent flow. *J Fluid Mech* 42:309-320
- Maaloe S (1978) The origin of rhythmic layering. *Mineral Mag* 42:337-345
- McBirney AR, Noyes RM (1979) Crystallization and layering of the Skaergaard Intrusion. *J Petrol* 20:487-554
- Nelson SA, Carmichael ISA (1979) Partial molar volumes of oxide components in silicate liquids. *Contrib Mineral Petrol* 71:117-124
- Nisbet EG, Fowler CMR (1978) The mid-Atlantic ridge at 37 and 45° N: some geophysical and petrological constraints. *Geophys JR Astron Soc Canada* 54:631-660
- O'Hara MJ (1968) The bearing of phase equilibria studies in synthetic and natural systems on the origin of evolution of basic and ultrabasic rocks. *Earth Sci Rev* 4:69-133
- O'Hara MJ (1977) Geochemical evolution during fractional crystallization of a periodically refilled magma chamber. *Nature* 266:503-507
- Rhodes JM, Dungan MA, Blanchard DP, Long PE (1977) Magma mixing at mid-ocean ridges: evidence from basalts drilled near 22° N on the mid-Atlantic ridge. *Tectonophysics* 55:35-62
- Rosendahl BR (1976) Evolution of ocean crust, 2. Constraints, implications and inferences. *J Geophys Res* 81:5305-5314
- Shaw HR (1972) Viscosities of magmatic silicate liquids: an empirical method of prediction. *Am J Sci* 272:870-893
- Sigurdsson H, Sparks RSJ (1978) Lateral magma flow within rifted Icelandic crust. *Nature* 274:126-130
- Smith RL (1979) Ash-flow magmatism. *Geol Soc Am, Spec Pap* 180:5-28
- Smewing JD Mixing characteristics and compositional differences in mantle-derived melts beneath spreading axes; evidence from cyclically layered rocks in the ophiolite of North Oman. *J Geophys Res* (in press)
- Sparks RSJ, Meyer P, Sigurdsson H (1980) Density variations amongst mid-ocean ridge basalts: Implications for magma mixing and the scarcity of primitive lavas. *Earth Planet Sci Lett* 46:419-430
- Sparks RSJ, Sigurdsson H, Wilson L (1977) Magma mixing: a mechanism of triggering acid explosive eruptions. *Nature* 267:315-318
- Stolper E, Walker D (1980) Melt density and the average composition of basalt. *Contrib Mineral Petrol* 74:7-12
- Thompson RN (1973) One atmosphere melting behaviour and nomenclature of terrestrial lavas. *Contrib Mineral Petrol* 40:197-204
- Townsend AA (1976) *The Structure of Turbulent Shear Flow*. Cambridge University Press
- Turner JS (1979) *Buoyancy Effects in Fluids*. Cambridge University Press
- Usselman TM, Hodge DS (1978) Thermal control of low-pressure fractionation processes. *J Volcan Geo Res* 4:265-281
- Wadsworth WJ (1961) The layered ultrabasic rocks of south-west Rhum, Inner Hebrides. *Philos Trans R Soc London B*244:21-64
- Wager LR, Brown GM (1968) *Layered Igneous Rocks*. Oliver Boyd, Edinburgh
- Wager LR, Deer WA (1939) Geological investigations in East Greenland, Part III. The petrology of the Skaergaard Intrusion, Kangerdugssuaq, East Greenland. *Medd Groenl* 105 (No. 4):1-352
- Walker D, Shibata T, Long SE (1979) Abyssal tholeiites from the Oceanographer Fracture Zone, II. Phase equilibria and mixing. *Contrib Mineral Petrol* 70:111-125